Marine Genomics

Bimodal distribution of seafloor microbiota diversity and function are associated with marine aquaculture

--Manuscript Draft--

Manuscript Number:	MARGEN-D-22-00051R2
Article Type:	Full Length Article
Section/Category:	Genomics/technical resources
Keywords:	16S rRNA; seafloor; microbiota; Marine; Aquaculture
Corresponding Author:	Knut Rudi NORWAY
First Author:	R. Pettersen
Order of Authors:	R. Pettersen
	I. Ormaasen
	I. L. Angell
	N. B. Keeley
	A. Lindseth
	L. Snipen
	Knut Rudi
Abstract:	The aim of the current work was to investigate the impact of marine aquaculture on seafloor biogeochemistry and diversity from pristine environments in the northern part of Norway. Our analytical approach included analyses of 182 samples from 16 aquaculture sites using 16S and 18S rRNA, shotgun analyses, visual examination of macro-organisms, in addition to chemical measurements. We observed a clear bimodal distribution of the prokaryote composition and richness, determined by analyses of 16S rRNA gene operational taxonomic units (OTUs). The high OTU richness cluster was associated with non-perturbed environments and farness from the aquaculture sites, while the low OTU richness cluster was associated with perturbed environments and proximity to the aquaculture sites. Similar patterns were also observed for eukaryotes using 18S rRNA gene analyses and visual examination, but without a bimodal distribution of OTU richness. Shotgun sequencing showed the archaeum Nitrosopumilus as dominant for the high OTU richness cluster, and the epsilon protobacterium Sulfurovum as dominant for the low OTU richness cluster. Metabolic reconstruction of Nitrosopumilus indicates nitrification as the main metabolic pathway. S ulfurovum , on the other hand, was associated with sulfur oxidation and denitrification. Changes in nitrogen and sulfur metabolism is proposed as a potential explanation for the difference between the high and low OTU richness clusters. In conclusion, these findings suggest that pollution from elevated loads of organic waste drives the microbiota towards a complete alteration of respiratory routes and species composition, in addition to a collapse in prokaryote OTU richness.
Suggested Reviewers:	sara kleindienst sara.kleindienst@uni-tuebingen.de
	William Orsi w.orsi@lrz.uni-muenchen.de
	Stilianos Louca louca@zoology.ubc.ca
Opposed Reviewers:	
Response to Reviewers:	

Cover letter

Dear Editor,

Please find our second revision of our manuscript entitled **“Bimodal distribution of seafloor microbiota diversity and function are associated with marine aquaculture”,** submitted for consideration.

We have now revised the manuscript, considering the comments by the editor and the reviewers. We hope that the manuscript is now suitable for MARGEN.

Sincerely yours,

Prof. Knut Rudi
Norwegian University of Life Sciences (NMBU)
Chemistry, Biotechnology and Food Science Department (IKBM), Campus Ås
Ås 1432, Norway
knut.rudi@nmbu.no

The original revision is shown in red, while the R1 revision is shown in green.

Reviewer #1: Thank you for addressing all my comments and questions in the revised manuscript.
Response: We thank the reviewer for this comment

Reviewer #2: I reviewed the initial submission of the manuscript and notice that the authors have done their best to respond to the comments of both reviewers and adapt the text. The manuscript is almost ready for submission. I have two remarks.
Line 220-221: Wouldn't it be logical that ecological differences are realized at the species level? Species sorting is important in community composition (https://doi.org/10.1073/pnas.0707200104).

Response: We agree that it is logical that the ecological differences should be realized at the species level. This information is now included in the revised manuscript (l. 222-223).

You use a metagenetic approach, but metagenomics is probably more appropriate. See https://doi.org/10.1038/s41592-018-0176-y

Response: We agree that a metagenomic approach would be preferable. The challenge with sediments, however, is the large diversity of uncharacterized microorganisms. This renders the metagenomic approach challenging, since important microorganisms can be overlooked. This is the reason why we used a metagenetic approach.

Line 382: please refer to the reason for including the human genome screen (as you did in the rebuttal letter) I still noticed a lot of typos, incomplete references, and a few figures which need additional information. My minor comments are included in the manuscript pdf attached.

Response: We thank the reviewer for the comments. We have now included the reason for the human genome screen in the revised manuscript (l. 382-383). We are sorry for the typos and incomplete references. The text has been corrected, and we have tried to update the references, which is challenging due to the different formats in the Endnote library. We have also included additional information to the figures, as required.

Revised MARGEN-D-22-00051_R1

Running Head: Seafloor microbiota in aquaculture

Bimodal distribution of seafloor microbiota diversity and function are associated with marine aquaculture

R. Pettersen[1], I. Ormaasen[2], I. L. Angell[2], N. B. Keeley[3], A. Lindseth[4], L. Snipen[2] and K. Rudi[2*]

[1]Akvaplan-niva, Tromsø, Norway [2]Norwegian University of Life Sciences, Ås, Norway

[3]Institute of Marine Research, Tromsø, Norway, [4]Aquakompetanse, Flatanger, Norway

*corresponding author knut.rudi@nmbu.no

Keywords: 16S rRNA, seafloor, microbiota, marine, aquaculture

ABSTRACT

The aim of the current work was to investigate the impact of marine aquaculture on seafloor biogeochemistry and diversity from pristine environments in the northern part of Norway. Our analytical approach included analyses of 182 samples from 16 aquaculture sites using 16S and 18S rRNA, shotgun analyses, visual examination of macro-organisms, in addition to chemical measurements. We observed a clear bimodal distribution of the prokaryote composition and richness, determined by analyses of 16S rRNA gene operational taxonomic units (OTUs). The high OTU richness cluster was associated with non-perturbed environments and farness from the aquaculture sites, while the low OTU richness cluster was associated with perturbed environments and proximity to the aquaculture sites. Similar patterns were also observed for eukaryotes using 18S rRNA gene analyses and visual examination, but without a bimodal distribution of OTU richness. Shotgun sequencing showed the archaeum *Nitrosopumilus* as dominant for the high OTU richness cluster, and the epsilon protobacterium *Sulfurovum* as dominant for the low OTU richness cluster. Metabolic reconstruction of *Nitrosopumilus* indicates nitrification as the main metabolic pathway. S*ulfurovum*, on the other hand, was associated with sulfur oxidation and denitrification. Changes in nitrogen and sulfur metabolism is proposed as a potential explanation for the difference between the high and low OTU richness clusters. In conclusion, these findings suggest that pollution from elevated loads of organic waste drives the microbiota towards a complete alteration of respiratory routes and species composition, in addition to a collapse in prokaryote OTU richness.

INTRODUCTION

Ecosystem functions are crucial for life on Earth, providing the oxygen in the atmosphere and essential carbon fixation services. Despite the fact that the sea covers about 70% of the earth's surface and contains approximately half of the planet's microbial biomass, the ecosystem services provided by the seafloor microbiota and the impact of anthropogenic activities on these services remain poorly understood (1-3). There are, however, alarming changes in seafloor ecosystem functioning with a 4-fold increase in dead zones since the 1950s, with deoxygenation representing one of the most important changes affecting marine ecosystems on a global scale (4).

A critical knowledge gap relates to the switch between oxic and anoxic respiration in marine sediments (5-7). Anoxic respiration can lead to the buildup of toxic gasses such as hydrogen sulfide and carbon dioxide. Denitrification represents the main anoxic respiration process in today's oceans (8). Although dinitrogen gas, the end product of denitrification, is non-toxic, there are several potentially toxic intermediates that could negatively affect marine food webs (9). Therefore, anthropogenic activities that promote benthic denitrification are potential threats to the stability of marine ecosystems.

Aquaculture is an important industry providing seafood to a growing worldwide market. However, the production is not emission free and often negatively impacts local faunal diversity, and contributes to the pollution of the oceans (10). In Norway, the aquaculture industry pollutes about twice that of the human population, representing a significant pollution source of the Norwegian fjords (11). Accumulation of organic waste such as fish food and excrement creates anoxic conditions and the production of hydrogen sulfide gas, affecting benthic functioning and life supporting capacity immediately beneath the net pens (12). This state is usually associated

with loss of benthic macro- and meiofauna biodiversity and profound changes in the sediment biogeochemical processes, in particular deoxygenation and hydrogen sulfide production due to the elevated load of organic material (13-15). Although the effects of organic enrichment have been well studied in the context of benthic geochemistry, there remain several knowledge gaps surrounding other potential drivers and thresholds for diversity loss (16).

The aim of the current work was to investigate how localized organic pollution at marine fish farm installations can be used to mirror the impact of anthropogenic activities on seafloor diversity and biochemical processes (11).

We used 16S rRNA gene and shotgun analyses, in addition to analyses of macrofauna and chemical composition, to obtain knowledge about biological processes in the sediments. For functional assignments we used a combination of taxonomic prediction and metabolic reconstruction. The rationale is that, in many cases, taxonomic associations will be superior to metabolic reconstruction in unveiling biochemical properties of microorganisms (17).

RESULTS

In total, 182 subsamples from 61 stations, sampled from 16 aquaculture locations were analyzed (Suppl Table 1). All samples were analyzed for the quantity and composition of both prokaryotes and eukaryotes through 16S and 18S rRNA genes, while shotgun sequencing was undertaken for 12 selected samples based on high and low OTU richness. A subset of 38 locations from 8 aquaculture sites were also analyzed for macrofauna and chemical composition (Suppl Table 4).

Microbiota quantity and diversity

Quantitative PCR revealed that the level of rRNA gene copies was 8.7±0.8 and 6.5±0.6 [mean±std] log10 copies/g for prokaryotes and eukaryotes, respectively. For the sequencing, we detected a total of 23,765 prokaryote and 7,887 eukaryote OTUs from all samples, with the OTU richness per sample ranging from 82 to 2,762 for prokaryotes and 15 to 347 for eukaryotes.

Bimodal distribution of prokaryote OTU richness

Prokaryotes showed a bimodal distribution with two peaks in OTU richness (p=0.008, Hartigan dip test). The low richness showed a peak at 601±314 [mean±std] and high OTU peak at 2,010±347 [mean±std] (Fig. 1A). A cutoff of 1250 OTUs was defined from the mean value of the histogram bar separating the high- and low OTU richness clusters (Fig 1A) The eukaryote OTU distribution, on the other hand, showed a unimodal distribution (p=0.55, Hartigan dip test), with a single peak at 237±113 [mean±std] species (Fig. 1B). Both the prokaryote and eukaryote beta-diversity revealed a separation based on the prokaryote high and low OTU richness cluster (Fig. 1C and D, respectively). In addition, there was also a relatively strong direct correlation between eukaryote – and prokaryote OTU richness (Spearman rho = 0.74, $p = 5.9^{-27}$). The eukaryote 18S rRNA gene copy number was higher for the high prokaryote OTU richness cluster compared to the low OTU richness cluster (6.6±0.8 vs 6.4±0.5 gene copies/g [mean±std for high and low prokaryote OTU richness cluster, respectively], p = 0.007, Kruskal Wallis test). Similar trends (although not statistically significant) were also detected with the 16S rRNA gene copy number (8.6±0.8 vs 8.7±0.9 gene copies/g [mean±std] for high and low prokaryote OTU richness cluster, respectively], p = 0.09, Kruskal Wallis test).

The prokaryote OTU richness clusters showed a statistically significant difference in distribution across the aquaculture sites (p = 0.009, Chi-square test). A clear positive correlation was observed with respect to distance from the aquaculture site. Low diversity clusters were

111 associated with the sites in close proximity to the cages and high OTU richness clusters being
112 overrepresented for the distant sites, while the intermediate distances were associated with
113 intermediate levels of OTU richness (Fig. 2). No clear differentiation in OTU richness was
114 observed according to geographical region, as visualized by geo-mapping of the samples with
115 geocoordinates (Fig. 1E).

116 **Taxonomic composition and predicted function of the microbiota**

117 The prokaryote OTUs belonged to 1,405 genera, of which 135 genera had a mean abundance
118 above 1 ‰, whereas the eukaryotic OTUs belonged to 555 genera, 40 of which had an
119 abundance above 1 ‰. *Sulfurovum* was the prokaryotic genus with the highest abundance (mean
120 abundance = 8.0 %, Fig. 3A), while for eukaryotes the dominant genus *Scipsiella* had a mean
121 abundance of 19.0 % (Fig. 3B). A volcano plot analyses (Fig. 3C) revealed that the prokaryote
122 genera *Sulfurovum* and *Christenella* were associated with the low OTU richness cluster, while
123 there were 14 genera associated with the high OTU richness cluster, including the archaeum
124 *Nitrosopumilus*. For the eukaryotes, the genera *Cryothecomonas, Ebria* and *Pterosperma* were
125 associated with low prokaryote OTU richness, while *Amastiggomonas, Gyrodinium* and
126 *Katablepharis* were associated with high OTU richness (Fig. 3D). Detailed taxonomic ranks are
127 given for prokaryotes in Suppl. Table 2, and for eukaryotes in Suppl. Table 3

128 There was a clear positive association between ammonium predicted as an electron donor
129 (nitrification) and high OTU richness (Fig. 4A), while carbon predicted as electron donor and
130 nitrogen as electron acceptor (heterotrophic denitrification) both shared a negative relationship
131 with OTU richness (Fig. 4B and C). The same trends were observed both for prokaryotes and for
132 eukaryotes (Fig. 4D to E), while the trends were stronger for prokaryotes. The other predicted
133 electron donors/acceptors (hydrogen, oxygen and sulfur) did not show similar strong correlations

with OTU richness (results not shown). All the predictions were done through the application of the FAPROTAX database (47).

Metagenome assembled genomes (MAGs) from high and low prokaryote OTU richness samples

Shotgun sequencing identified *Nitrosopumilus* as the dominant taxon for the high OTU richness cluster, while *Sulfurovum* was dominant for the low OTU richness cluster (Fig. 5A). Shotgun sequencing also revealed differences in both the functional and the process annotations between the high and low OTU richness clusters (Fig 5B). Notably, hydrolysis and proteolytic activity were associated with the high diversity cluster, while the low diversity cluster showed an association with transferases and redox electron transfer chains (Fig. 5 C and D).

We collectively identified 259 bins using maxbin and metabat (Suppl. Table 5). dRep quality filtering and clustering in 13 bins of superb quality that clustered into 5 unique MAGs. Two of these MAGs belong to the genus *Sulfurovum*, while none belonged to *Nitrosopumilus* despite its prevalence in all the high OTU richness samples, as determined by kaiju. Therefore, in order to investigate *Nitrosopumilus* we collected all the bins classified as *Nitrosopumilus* by GTDBTk (18), regardless of dRep filtering (19). All high richness samples contained one such bin, but sample 34 contained two. These were merged into one pangenome, and the same was done for the *Sulfuroum* MAGs, resulting in another pangenome. These pangenomes were selected for further functional annotation due to their overall dominance in the high and low OTU richness cluster, respectively.

The *Nitrosopumilus* pangenome revealed 15,627 predicted genes, while the *Sulfurovum* pangenome contained 29,513 genes. The main differences between the pangenomes were related

to vitamin B_{12} synthesis, carbon fixation, nitrogen- and sulfur metabolism. *Nitrosopumilus* showed the potential for several important functions: vitamin B_{12} production through the presence of *cbi* and *cob genes*, nitrification with the presence of the B12 containing *mcm* gene, sulfur reduction driven by the *sat* gene, and nitric oxide- and hydrogen sulfide production through the *sir* gene (Fig. 6A). *Sulfurovum*, on the other hand, lacked the genes for vitamin B12 production and contained the genes *soxY and soxC* connected to sulfur oxidation, and the genes *cysH* and *sat* connected to sulfur reduction. *Sulfurovum* also contained the denitrification gene *norB*, with nitrous oxide as the main end-product. *Sulfurovum* could also potentially fix CO_2 through a reductive TCA cycle through the possession of 2-ketoglutarate:ferredoxin oxidoreductase (KGOR) for fixing CO_2 and the *leuA* gene for generating acetyl-CoA (Fig. 6B).

OTU richness associations with chemical composition

The organic carbon levels in the sediments ranged from 1.4. to 6.0%, while the levels of nitrogen were between 0.03 and 0.6% (Suppl. Table 4). A statistically significant correlation existed between organic carbon levels and prokaryote OTU richness (Fig. 7A). The high and low OTU richness clusters showing the strongest associations were separated at an organic carbon level of 2.1%, indicating a possible environmental threshold for OTU richness (Fig. 7B). For organic carbon levels below 2.1% the high OTU cluster showed a 2.5-fold higher prevalence than expected by chance, while the prevalence was half of the prevalence expected by chance for levels above 2.1%. By partial least squares modelling in latent variables (PLS) we also observed a direct association between the microbiota composition and TOC (Fig 7C). The genera *Sulforovum* and *Christensenella* (identified as statistically significant associated with the low OTU richness cluster), in addition to the anaerobic fermenting *Petrocella* (20) and the sulfidogenic *Desulforhopalus* (21) were associated with high organic carbon. *Nitropumilus*

(indicative of high OTU richness cluster) was associated with low organic carbon, in addition to *Ferruginivarius* and the autotrophic sulfate oxidizer *Thiogranum* (22). For total nitrogen we did not identify statistically significant associations with prokaryote OTU richness for any level of nitrogen ($p > 0.05$, Chi-square test). The direct association between total nitrogen and the OTU composition was also very low, with R^2=0.24 and 0.006 for calibrated and cross validated PLS, respectively.

OTU richness associations with macrofauna indexes

All the macrofauna indices were highly correlated with OTU richness (> 0.75, Spearman rho), with H' showing the largest span (> 20-fold difference from the lowest to the highest measure, Suppl. Table |4). The macrofauna indexes based on fauna ecological classification groupings were especially strongly correlated, exhibiting consistent positive correlations with high prokaryote OTU richness, with ES100 (estimated number of macroscopic species in a random subset of 100 individuals) showing the strongest association (Fig. 8). Unfortunately, we did not have access to the underlying raw count-data that was used to derive the macrofauna diversity indices.

DISCUSSION

We found a clear bimodal distribution in prokaryote OTU richness. To our knowledge, our study is the first to unveil such pattern. The low and high OTU richness cluster showed a strong association with proximity to aquaculture sites, but no systematic association with geographic distribution. The changes with respect to proximity to the farms were most likely driven by elevated levels of organic bio-deposits (fish and feed waste), with the associated benthic organic

enrichment and oxygen depletion (13, 23). There was evidence that this occurs at an organic carbon threshold of 2.1%, which corresponds to a relatively low level / early stages of enrichment, as highly enriched sediment directly beneath farms can exceed 15 % organic carbon (24). Therefore, the low OTU richness cluster probably reflects several different environmental states correlating with the gradient of organic carbon (25, 26). The high OTU cluster, on the other hand, showed a surprising homogenous distribution across a wide range of locations.

By taxonomic prediction, the low diversity cluster was predicted to be correlated to organic carbon as an electron donor and nitrogen as electron acceptor (anoxic denitrifying respiration), while the high diversity cluster was predicted to be correlated to nitrification involving CO_2 fixation and nitrogen oxidation. Nitrification and denitrification reduction have opposing effects on organic carbon flux, with nitrification leading to assimilation, while denitrification/sulfate reduction leads to mineralization of carbon. Since completely different microbial assemblages are associated with nitrification and denitrification (27), both the difference in composition and function of the microbiota for the high and low OTU richness cluster could be related to electron transport chains.

As well as identifying potential electron donors and acceptors in the low diversity cluster, shotgun analyses indicated the importance of hydrolysis and proteolysis within the high diversity cluster, while transferases were overrepresented in the low diversity cluster. Both properties can be provided by the genera *Pseudomonas* and *Streptomyces*, which are highly abundant in both the high and low OTU richness cluster. In particular, *Streptomyces* is important for aerobic recycling of organic material (28, 29). This may indicate that ecological differences related to degradation of organic material are not reflected at the genus level, but need species level resolution be revealed (30). Previously, a biphasic distribution of proteolytic activity connected

to organic carbon load has also been observed for benthic marine sediments, suggesting the importance of polymer degradation in benthic communities (31). The functionality of the dominant species for the high and the low diversity clusters further supports major differences in biogeochemical processes, with the dominant archaeum *Nitrosopumilus*, as revealed by shotgun sequencing, being both a nitrifying and CO_2 fixing microorganism (32). We found the enzymatic machinery for vitamin B_{12} production as a cofactor for methylmalonyl-CoA mutase (mcm), being essential for carbon fixation through the hydroxypropionate (HP) cycle (33). Vitamin B_{12} producing archaeum have been proposed as crucial for global production in marine environments (34). Interestingly, dominant genus *Sulforovum* in the low diversity cluster prefers enrichments with a high hydrogen sulfide to oxygen ratio (35). Furthermore, *Sulurovum* seems to lack genes to reduce nitrous oxide to dinitrogen. Nitrous oxide is a potent inactivator of B_{12} (36, 37). Therefore, a potential consequence could be that *Sulforovum* inhibits the essential carbon fixation by *Nitrosopumilus* through nitrous oxide emission. This observation would be consistent with the high levels of ammonium that can be emitted from heavily polluted sediments (13, 23).

A candidate service could relate to the ability to produce vitamin B_{12}, which is extremely costly and confined to a limited number of bacteria and archaea (34). Since vitamin B_{12} is essential for carbon fixation by archaeum in sediments with low organic carbon load, it is possible that the carbon fixation process itself is the driver for B_{12} production; in effect, fortifying the trophic chain with this essential vitamin. On the contrary, nitrous oxide emission by denitrifying bacteria could inhibit essential B_{12}-dependent enzymatic activities such as isomerases, methyltransferases and dehalogenases (38). This could potentially contribute to the prokaryote diversity loss for the communities driven by denitrification and potential macrofauna diversity loss by lack of trophic chain fortification.

247 The majority of the prokaryote OTUs that were unique to the high OTU richness cluster belongs
248 to cosmopolitan marine OTUs. Four of the OTUs belong to cosmopolitan uncultured JTB255-
249 Marine Benthic Group (39, 40). The most discriminant BD7-8 marine group has recently been
250 shown to have strong correlations with burrowing eukaryotes, potentially utilizing
251 electrochemical gradients in sediments (41). *Desulfobulbus*, which also was among the 10 most
252 discriminatory OTUs, has the ability to utilize electrochemical gradients through external
253 electron transfer (42). The cosmopolitan ammonium oxidizing archaeum *Nitrosopumilus* has the
254 ability to utilize ammonium down to levels that can barely sustain life (43), in addition to being
255 highly efficient in carbon fixation (32, 44). The tight clustering of the high OTU rich
256 communities may indicate that there is a limited number of ways that biological activities can be
257 sustained under these conditions. This may also indicate low resilience and high vulnerability of
258 the high OTU richness cluster towards perturbations by anthropogenic activities.

259 The bacteria associated with the low OTU richness cluster did not show a homogenous
260 distribution pattern across the samples. Only the genera *Sulfurovum* and *Christensenella* were
261 consistently associated with the low richness cluster, suggesting that disturbances driven by high
262 organic loading can lead to different community assemblages. The low OTU richness cluster
263 probably reflects several different environmental states, as the threshold of 2.1% organic carbon
264 that appeared to distinguish high and low OTU richness communities corresponds to a low to
265 moderately enriched benthic state. Highly enriched sediments can be associated with total
266 organic contents in excess of 15% and it has also been established the bacteria form a strong
267 transitional gradient in response to enrichment (through space of time) (25, 26). This pattern is in
268 line with our general understanding of microbial ecology, where environmental filtering (45) can
269 lead to several different states (46). Interestingly, both nitric oxide (47) and hydrogen sulfide

(48) can cause DNA damage, providing potential explanations for DNA repair enzymes being associated with the low OTU richness cluster. Unfortunately, we did not include measurements of redox potential, hydrogen sulfide and oxygen that could have revealed more detailed associations for the low OTU richness cluster.

For the macrofauna indexes, ES100 had the strongest association with the prokaryote OTU richness. Since ES100 is a sample size independent proxy of species richness, the positive correlation indicates a strong positive link between prokaryote and macroscopic eukaryote species richness. This observation is consistent with Keeley et al. (23), which demonstrated analogous compositional changes in response to enrichment for eukaryotes via eDNA and via visual taxonomy and for bacteria. We also identified a statistically significant reduction in eukaryote 18S rRNA gene copy number for the prokaryote low OTU richness cluster. These findings further support that the low prokaryote OTU richness cluster is associated with conditions that are detrimental to macroscopic eukaryotes (49). The strong association of the bimodal distribution of prokaryote OTU richness with macrofauna, may indicate that prokaryote OTU richness could represent a new parameter for environmental surveillance. The taxonomic difference between the high – and low OTU richness clusters may facilitate the identification of indicator taxa for diagnostic purposes, allowing the development of rapid, targeted diagnostic approaches (50).

In conclusion, we found a surprising bimodal species richness distribution connected to anthropogenic activity. The high diversity cluster seemed to be associated with nitrification, while the low diversity cluster seemed to be associated with denitrification. Functional associations also indicate that the high species richness cluster also could contribute with

community services such as B_{12} production. The existence of seafloor microbiota tipping points can have major implications for future management of marine resources.

MATERIALS AND METHODS

Study sites

Sampling for e-DNA was conducted in conjunction with routine environmental investigation of 16 marine farms (called C-investigations in Norway), with parallel samples being obtained from the same grabs that were taken (Fig. 9). The aim of the C- investigations is to assess the level of organic enrichment from the fish farm on the surrounding marine environment. Sampling stations were situated close to, midway and far from the aquaculture sites, representing heavily impacted-, intermediately impacted-, and non-impacted regions.

Macrofauna analyses

The macrofauna and chemical analyses were conducted according to requirements from the Norwegian authorities (51). The softbottom macrofauna samples were collected using a 0.1 m^2 Van Veen grab. At each station, two replicates (0.4 m^2) for macrofaunal analyses were sieved through a 1 mm round mesh sieve, preserved in a 4% borax-buffered formaldehyde solution stained with rose bengal, and stored in plastic buckets. Only samples with undisturbed sediment surface and perfect closure of the grab were accepted. The sampling procedure was carried out in accordance with ISO 16665:2014. Preserved samples were shipped to the laboratory for sorting, quantification, and identification to lowest taxonomical level (species) when possible by a qualified taxonomist. Quantified species lists were used for the statistical analysis, and different indices were used for highlighting the different aspects of faunal community. The indexes used were the Shannon-Wiener diversity index (H), Hulbert diversity index (ES_{100}), Norwegian

sensitivity index (NSI), indicator species index (ISI2012) and the Norwegian quality index (NQl1) (52).

Chemical analyses

From one Van Veen grab sample per station, sample material was collected from the upper 1 cm of the undisturbed sediment surface by inserting a spoon through the inspection hatch of the grab. The sediment samples were frozen at -20 °C for shipment and further processing in the laboratory. In the laboratory, sediments were analyzed for Total Organic Carbon (TOC), in addition to total nitrogen (51). TOC was calculated after drying sediment samples at 40 °C. Calculations were based on weight loss after combustion at 495 °C, according to DIN19539:2016 (53).

Sediment sampling for microbiota analyses

From one Van Veen grab sample approximately 1 gram of surface sediment was collected from three different locations on each grab using a sterile spoon (Sarstedt, Germany) and placed in tubes containing 3 ml S.T.A.R buffer (Roche, Germany) to stabilize the samples for room temperature shipment. The samples were sent by mail at room temperature to the laboratory at the collection day or the day after collection, with the shipment taking 2 to 3 days. If the samples could not be sent within this timespan, they were stored in a refrigerator. Upon arrival at the laboratory the samples were stored at -20 °C and processed within 1 month.

DNA Extraction

First, the sediment samples were thawed and homogenized by vortexing, and then DNA from a 250 µl sample was extracted with the MagAttract PowerSoil DNA KF Kit. The extraction was performed according to the manufacturer's instructions except on the two following points: (1)

Mechanical lysis was achieved by four rounds of shaking in a FastPrep96 instrument (MP Biomedicals, France) for 30 s at 1800 rpm. (2) To avoid particles in the supernatant, the volume retrieved after the second centrifugation was 750 µl. DNA concentration was determined with the Qubit dsDNA HS Assay Kit (Thermo Fisher Scientific, USA). The quantification was preformed according to the manufacturer's instructions, using 2 µl template.

Quantitative PCR

Quantification of prokaryote and eukaryote DNA was done as previously described, using the PRK341F/PRK806R and 3NDF /V4EukR2 primer pairs, respectively(54) . The qPCR conditions involved initial denaturation at 95°C for 15 min, followed by 40 cycles of denaturation at 95°C for 30 s, annealing at 55/59°C (prokaryote/eukaryote) for 30 s, and elongation at 72°C for 45/30 s (Prokaryote/Eukaryote). Two microliter template and 200 nM of each primer were used for amplification in a 1 × Hot FirePol EvaGreen qPCR Supermix (Solis BioDyne, Tartu, Estonia). The qPCR was conducted using the CFX96 Touch™ Real-Time PCR Detection System (Bio-Rad, USA). Quantitative information was derived using standard curves. The determined amplification efficiencies were 0.69/0.88 (Prokaryote/Eukaryote), with squared regression coefficient > 0.99 for both.

Amplicon sequencing

A two-step PCR amplification was carried out as previously described using the primer pairs PRK341F/PRK806R targeting the V3–V4 region of the prokaryotic SSU gene, and 3NDF /V4EukR2 targeting the V4 region of the eukaryotic SSU gene (54). Sequencing was performed on a MiSeq platform (Illumina, CA, USA) using a V3 chemistry kit for 300 bp paired-end reads. Resulting reads were joined and demultiplexed before quality filtering where singletons were

removed; min length was set to 350 and maxEE = 1.0. Clustering was done using the UPARSE algorithm with ≥ 97% similarity, as implemented in USEARCH 8.0. Taxonomy was assigned with the SINTAX classifier, using the RDP 16s rRNA training set 18f or prokaryotes and SILVA v123 eukaryotic 18S subset for eukaryotes (55). Prokaryote and eukaryote datasets were rarefied at 10,000 and 5,000 sequences, respectively.

Each of the OTUs was subsequently matched to the Functional Annotation of Prokaryotic Taxa (FAPROTAX) database (56) through sequence homology at the 97% level. For the beta diversity analyses, we used Bray-Curtis distances with PCoA visualization, and statistical significance for cluster associations using Anosim, as implemented in the FANTOM package (57).

Shotgun sequencing

Shotgun sequencing was used to identify and characterize the dominant species associated with the high and low OTU richness cluster. Twelve samples (6 high and 6 low OTU richness) were selected for in-depth analyses by shotgun sequencing to determine the association of the OTU richness clusters. The high OTU richness group included samples with >1250 OTUs, while low OTU richness group included samples with < 1250 OTUs.

The Illumina DNA Prep kit (Illumina, USA) was used in the sample preparation for whole genome sequencing. The DNA (1-10 ng) was fragmented, tagged with adapter sequences and amplified according to the manufacturer's recommendations. The amplified libraries were purified with a 1.8 × purification bead solution volume to sample volume. Quantification of the libraries was performed using Qubit dsDNA HS Assay Kit (Thermo Fischer Scientific, USA), following the manufacturer's instructions for 2 µl sample. The libraries were normalized into one

sequencing pool and then sequenced at the Norwegian Sequencing Centre (NSC, Oslo, Norway) on one lane of a HiSeq4000 platform (Illumina, USA), yielding 150 bp paired-end reads.

Shotgun data were first quality filtered and trimmed using BBduk (BBmap v38.86) (58). Next, all reads were mapped against the human genome with bowtie2 v2.4.1 (59) due to Norwegian legislation, and non-mapping reads were collected with samtools v1.9 (60) as a de-contamination step. Paired-end reads were merged with BBmerge (BBmap v38.86) (58), and both merged and non-merged (still as pairs) were used as input to SPAdes (metaspades) v3.14 for assembly (61). Assembled contigs were binned both by maxbin v2.2.7 (62) and metabat2 v2.15 (63), and all resulting bins were finally grouped and quality checked by dRep v.2.6.2 (19). All bins, regardless of dRep, were given a taxonomic classification using GTDBTk v1.3.0 (18).

Gene identification was done using the Find Prokaryotic Gene module, while functional annotations were conducted using the EggNOG pipeline (64) in the CLC genomic workbench (Qiagen, Hilden, Germany). Both the gene identification and annotation were performed using default parameters. In addition to this, raw shotgun reads were also subject to a taxonomic classification, using the kaiju software (65) with the non-redundant (nr) protein database from NCBI. The choice was motivated by the presumption that sea sediments contain many less described organisms, making protein similarities a more sensitive criterion for finding similar taxa in the database.

Statistical analyses

Statistical analyses were done in the Matlab r2020a programming environment (MathWorks Inc, Natic, USA), using the PLS toolbox plugin (Eigenvector Inc, Washington, USA) for multivariate statistical analyses. Hartigan's dip test was used to evaluate the bimodality of the OTU richness

distribution (66). Regression analyses were performed using the non-parametric Spearman correlation, while categorical associations were determined using the chi square test. The volcano plots were generated using Matlab, using p-values derived from the Kruskal-Wallis test.

Data availability

The raw sequencing data are available in the NCBI SRA database under the accession # PRJNA733024.

ACKNOWLEDGEMENTS

We thank the technical staff at Akvaplan-niva and Aqua kompetanse AS for conducting the sampling. The work was supported by the Norwegian regional research grant # RFF 285266, and the Norwegian Research Council grant # 320076.

COMPETING INTERESTS

None of the authors have competing interest to declare.

REFERENCES

1. Kallmeyer J, Pockalny R, Adhikari RR, Smith DC, D'Hondt S. 2012. Global distribution of microbial abundance and biomass in subseafloor sediment. 109:16213-16216.
2. Thurber A, Sweetman A, Narayanaswamy B, Jones D, Ingels J, Hansman R. 2014. Ecosystem function and services provided by the deep sea. Biogeosciences 11:3941–3963.
3. Manuel P, Cruz L, Carrasco P. 2021. The Knowledge Status of Coastal and Marine Ecosystem Services - Challenges, Limitations and Lessons Learned From the Application of the Ecosystem Services Approach in Management. Frontiers in Marine Science 8:27.
4. Breitburg D, Levin LA, Oschlies A, Grégoire M, Chavez FP, Conley DJ, Garçon V, Gilbert D, Gutiérrez D, Isensee K, Jacinto GS, Limburg KE, Montes I, Naqvi SWA, Pitcher GC, Rabalais NN, Roman MR, Rose KA, Seibel BA, Telszewski M, Yasuhara M, Zhang J. 2018. Declining oxygen in the global ocean and coastal waters. Science 359:eaam7240.
5. Kump L, Pavlov A, Arthur M. 2005. Massive release of hydrogen sulfide to the surface ocean and atmosphere during intervals of oceanic anoxia. Geology 33:397-400..
6. Dakos V, Matthews B, Hendry AP, Levine J, Loeuille N, Norberg J, Nosil P, Scheffer M, De Meester L. 2019. Ecosystem tipping points in an evolving world. Nature Ecology & Evolution 3:355-362.
7. Orsi WD. 2018. Ecology and evolution of seafloor and subseafloor microbial communities. Nature Reviews Microbiology 16:671-683.
8. Deutsch C, Sarmiento JL, Sigman DM, Gruber N, Dunne JP. 2007. Spatial coupling of nitrogen inputs and losses in the ocean. Nature 445:163-167.

9. Luypaert T, Hagan JG, McCarthy ML, Poti M. 2020. Status of Marine Biodiversity in the Anthropocene, p 57-82. *In* Jungblut S, Liebich V, Bode-Dalby M (ed), YOUMARES 9 - The Oceans: Our Research, Our Future: Proceedings of the 2018 conference for YOUng MArine RESearcher in Oldenburg, Germany doi:10.1007/978-3-030-20389-4_4. Springer International Publishing, Cham.

10. Schwitzguébel J-P, Wang H. 2007. Environmental impact of aquaculture and countermeasures to aquaculture pollution in China. Environmental Science and Pollution Research 14:452-462.

11. Olaussen JO. 2018. Environmental problems and regulation in the aquaculture industry. Insights from Norway. Marine Policy 98:158-163.

12. Holmer M, Kristensen E. 1992. Impact of Marine Fish Cage Farming on Metabolism and Sulfate Reduction of Underlying Sediments. Marine Ecology Progress Series 80:191-201.

13. Valdemarsen T, Bannister RJ, Hansen PK, Holmer M, Ervik A. 2012. Biogeochemical malfunctioning in sediments beneath a deep-water fish farm. Environ Pollut 170:15-25.

14. Mirto S, Gristina M, Sinopoli M, Maricchiolo G, Genovese L, Vizzini S, Mazzola A. 2012. Meiofauna as an indicator for assessing the impact of fish farming at an exposed marine site. Ecological Indicators 18:468-476.

15. Ingels J, Vanreusel A, Pape E, Pasotti F, Macheriotou L, Arbizu PM, Sørensen MV, Edgcomb VP, Sharma J, Sánchez N, Homoky WB, Woulds C, Leduc D, Gooday AJ, Pawlowski J, Dolan JR, Schratzberger M, Gollner S, Schoenle A, Arndt H, Zeppilli D. 2020. Ecological variables for deep-ocean monitoring must include microbiota and meiofauna for effective conservation. Nature Ecology & Evolution 5: 27-29.

16. Hillebrand H, Donohue I, Harpole WS, Hodapp D, Kucera M, Lewandowska AM, Merder J, Montoya JM, Freund JA. 2020. Thresholds for ecological responses to global change do not emerge from empirical data. Nature Ecology & Evolution 4:1502-1509.

17. Noronha A, Modamio J, Jarosz Y, Guerard E, Sompairac N, Preciat G, Danielsdottir AD, Krecke M, Merten D, Haraldsdottir HS, Heinken A, Heirendt L, Magnusdottir S, Ravcheev DA, Sahoo S, Gawron P, Friscioni L, Garcia B, Prendergast M, Puente A, Rodrigues M, Roy A, Rouquaya M, Wiltgen L, Zagare A, John E, Krueger M, Kuperstein I, Zinovyev A, Schneider R, Fleming RMT, Thiele I. 2019. The Virtual Metabolic Human database: integrating human and gut microbiome metabolism with nutrition and disease. Nucleic Acids Res 47:D614-D624.

18. Chaumeil P-A, Mussig AJ, Hugenholtz P, Parks DH. 2019. GTDB-Tk: a toolkit to classify genomes with the Genome Taxonomy Database. Bioinformatics 36:1925-1927.

19. Olm MR, Brown CT, Brooks B, Banfield JF. 2017. dRep: a tool for fast and accurate genomic comparisons that enables improved genome recovery from metagenomes through de-replication. The ISME Journal 11:2864-2868.

20. Quéméneur M, Erauso G, Frouin E, Zeghal E, Vandecasteele C, Ollivier B, Tamburini C, Garel M, Ménez B, Postec A. 2019. Hydrostatic Pressure Helps to Cultivate an Original Anaerobic Bacterium From the Atlantis Massif Subseafloor (IODP Expedition 357): *Petrocella atlantisensis* gen. nov. sp. nov. Front Microbiol 10:1497.

21. Lie TJ, Clawson ML, Godchaux W, Leadbetter ER. 1999. Sulfidogenesis from 2-aminoethanesulfonate (taurine) fermentation by a morphologically unusual sulfate-reducing bacterium, Desulforhopalus singaporensis sp. nov. Appl Environ Microbiol 65:3328-34.

22. Mori K, Suzuki KI, Yamaguchi K, Urabe T, Hanada S. 2015. Thiogranum longum gen. nov., sp. nov., an obligately chemolithoautotrophic, sulfur-oxidizing bacterium of the family Ectothiorhodospiraceae isolated from a deep-sea hydrothermal field, and an emended description of the genus Thiohalomonas. Int J Syst Evol Microbiol 65:235-241.

23. Keeley N, Valdemarsen T, Woodcock S, Holmer M, Husa V, Bannister R. 2019. Resilience of dynamic coastal benthic ecosystems in response to large-scale finfish farming. Aquaculture Environment Interactions 11: 161-179.

24. Hargrave B, Phillips G, Doucette L, White M, Milligan T, Wildish D, Cranston R. 1997. Assessing benthic impacts of organic enrichment from marine aquaculture, p 641-650, The Interactions Between Sediments and Water. Springer.

25. Keeley N, Wood SA, Pochon X. 2018. Development and preliminary validation of a multi-trophic metabarcoding biotic index for monitoring benthic organic enrichment. Ecological Indicators 85:1044-1057.

26. Quero GM, Ape F, Manini E, Mirto S, Luna GM. 2020. Temporal Changes in Microbial Communities Beneath Fish Farm Sediments Are Related to Organic Enrichment and Fish Biomass Over a Production Cycle. Frontiers in Marine Science 7:1-12.

27. Angell IL, Bergaust L, Hanssen JF, Aasen EM, Rudi K. 2020. Ecological Processes Affecting Long-Term Eukaryote and Prokaryote Biofilm Persistence in Nitrogen Removal from Sewage. Genes (Basel) 11: 1-14.

28. Busche T, Tsolis KC, Koepff J, Rebets Y, Rückert C, Hamed MB, Bleidt A, Wiechert W, Lopatniuk M, Yousra A, Anné J, Karamanou S, Oldiges M, Kalinowski J, Luzhetskyy A, Economou A. 2018. Multi-Omics and Targeted Approaches to Determine the Role of Cellular Proteases in Streptomyces Protein Secretion. Frontiers in Microbiology 9: 1-12.

29. Meng L, Zhang Y, Liu H, Zhao S, Wang J, Zheng N. 2017. Characterization of Pseudomonas spp. and Associated Proteolytic Properties in Raw Milk Stored at Low Temperatures. Frontiers in microbiology 8:2158-2158.

30. Van der Gucht K, Cottenie K, Muylaert K, Vloemans N, Cousin S, Declerck S, Jeppesen E, Conde-Porcuna J-M, Schwenk K, Zwart G, Degans H, Vyverman W, De Meester L. 2007. The power of species sorting: Local factors drive bacterial community composition over a wide range of spatial scales. Proceedings of the National Academy of Sciences 104:20404-20409.

31. Tholosan O, Lamy F, Garcin J, Polychronaki T, Bianchi A. 1999. Biphasic Extracellular Proteolytic Enzyme Activity in Benthic Water and Sediment in the Northwestern Mediterranean Sea. Applied and Environmental Microbiology 65:1619-1626.

32. Könneke M, Schubert DM, Brown PC, Hügler M, Standfest S, Schwander T, Schada von Borzyskowski L, Erb TJ, Stahl DA, Berg IA. 2014. Ammonia-oxidizing archaea use the most energy-efficient aerobic pathway for CO₂ fixation. Proceedings of the National Academy of Sciences 111:8239-8244.

33. Hügler M, Fuchs G. 2005. Assaying for the 3-hydroxypropionate cycle of carbon fixation. Methods Enzymol 397:212-21.

34. Doxey AC, Kurtz DA, Lynch MDJ, Sauder LA, Neufeld JD. 2015. Aquatic metagenomes implicate Thaumarchaeota in global cobalamin production. The ISME journal 9:461-471.

35. Hamilton T, Jones D, Schaperdoth I, Macalady J. 2014. Metagenomic insights into S(0) precipitation in a terrestrial subsurface lithoautotrophic ecosystem. Frontiers in microbiology 5: 1-16.

36. Stockton L, Simonsen C, Seago S. 2017. Nitrous oxide-induced vitamin B12 deficiency. Proceedings (Baylor University Medical Center) 30:171-172.

37. Sullivan MJ, Gates AJ, Appia-Ayme C, Rowley G, Richardson DJ. 2013. Copper control of bacterial nitrous oxide emission and its impact on vitamin B12-dependent metabolism. Proceedings of the National Academy of Sciences of the United States of America 110:19926-19931.

38. Richter N, Zepeck F, Kroutil W. 2015. Cobalamin-dependent enzymatic O-, N-, and S-demethylation. Trends in Biotechnology 33:371-373.

39. Mussmann M, Pjevac P, Kruger K, Dyksma S. 2017. Genomic repertoire of the Woeseiaceae/JTB255, cosmopolitan and abundant core members of microbial communities in marine sediments. ISME J 11:1276-1281.

40. Hoffmann K, Bienhold C, Buttigieg PL, Knittel K, Laso-Pérez R, Rapp JZ, Boetius A, Offre P. 2020. Diversity and metabolism of Woeseiales bacteria, global members of marine sediment communities. The ISME Journal 14:1042-1056.

41. Deng L, Bölsterli D, Kristensen E, Meile C, Su C-C, Bernasconi SM, Seidenkrantz M-S, Glombitza C, Lagostina L, Han X, Jørgensen BB, Røy H, Lever MA. 2020. Macrofaunal control of microbial community structure in continental margin sediments. Proceedings of the National Academy of Sciences 117:15911-15922.

42. Holmes DE, Bond DR, Lovley DR. 2004. Electron transfer by Desulfobulbus propionicus to Fe(III) and graphite electrodes. Appl Environ Microbiol 70:1234-7.

43. Martens-Habbena W, Berube PM, Urakawa H, de la Torre JR, Stahl DA. 2009. Ammonia oxidation kinetics determine niche separation of nitrifying Archaea and Bacteria. Nature 461:976-979.

44. Wuchter C, Abbas B, Coolen MJL, Herfort L, van Bleijswijk J, Timmers P, Strous M, Teira E, Herndl GJ, Middelburg JJ, Schouten S, Sinninghe Damsté JS. 2006. Archaeal nitrification in the ocean. Proceedings of the National Academy of Sciences 103:12317-12322.

45. Hanashiro FTT, De Meester L, Vanhamel M, Mukherjee S, Gianuca AT, Verbeek L, van den Berg E, Souffreau C. 2022. Bacterioplankton Assembly Along a Eutrophication Gradient Is Mainly Structured by Environmental Filtering, Including Indirect Effects of Phytoplankton Composition. Microb Ecol on line

46. Zaneveld JR, McMinds R, Vega Thurber R. 2017. Stress and stability: applying the Anna Karenina principle to animal microbiomes. Nature Microbiology 2:17121.

47. Burney S, Caulfield JL, Niles JC, Wishnok JS, Tannenbaum SR. 1999. The chemistry of DNA damage from nitric oxide and peroxynitrite. Mutat Res 424:37-49.

48. Attene-Ramos MS, Nava GM, Muellner MG, Wagner ED, Plewa MJ, Gaskins HR. 2010. DNA damage and toxicogenomic analyses of hydrogen sulfide in human intestinal epithelial FHs 74 Int cells. Environ Mol Mutagen 51:304-14.

49. Bonaglia S, Marzocchi U, Ekeroth N, Brüchert V, Blomqvist S, Hall POJ. 2019. Sulfide oxidation in deep Baltic Sea sediments upon oxygenation and colonization by macrofauna. Marine Biology 166:149.

50. Casen C, Vebo HC, Sekelja M, Hegge FT, Karlsson MK, Ciemniejewska E, Dzankovic S, Froyland C, Nestestog R, Engstrand L, Munkholm P, Nielsen OH, Rogler G, Simren M, Ohman L, Vatn MH, Rudi K. 2015. Deviations in human gut microbiota: a novel diagnostic test for determining dysbiosis in patients with IBS or IBD. Aliment Pharmacol Ther 42: 71-83.

51. Iversen A, Sandøy S. 2018. Veileder 02:2018 Klassifisering av miljøtilstand i vann. Økologisk og kjemisk klassifiseringssystem for kystvann, grunnvann, innsjøer og elver.,
52. Rygg B, Norling K. 2013. REPORT SNO 6475-2013 Norwegian Sensitivity Index (NSI) for marine macroinvertebrates, and an update of Indicator Species Index (ISI).
53. (DIN) DIfNEV. 2016. Investigation of solids - Temperature-dependent differentiation of total carbon (TOC400, ROC, TIC900).
54. Angell IL, Hanssen JF, Rudi K. 2017. Prokaryote species richness is positively correlated with eukaryote abundance in wastewater treatment biofilms. Lett Appl Microbiol 65:66-72.
55. Edgar RC. 2016. SINTAX: a simple non-Bayesian taxonomy classifier for 16S and ITS sequences. bioRxiv.
56. Louca S, Parfrey LW, Doebeli M. 2016. Decoupling function and taxonomy in the global ocean microbiome. Science 353:1272-1277.
57. Sanli K, Karlsson FH, Nookaew I, Nielsen J. 2013. FANTOM: Functional and taxonomic analysis of metagenomes. BMC Bioinformatics 14:38.
58. Bushnell B, Rood J, Singer E. 2017. BBMerge – Accurate paired shotgun read merging via overlap. PLOS ONE 12: 1-15
59. Langmead B, Salzberg SL. 2012. Fast gapped-read alignment with Bowtie 2. Nat Methods 9:357-9.
60. Li H. 2011. A statistical framework for SNP calling, mutation discovery, association mapping and population genetical parameter estimation from sequencing data. Bioinformatics 27:2987-93.

61. Nurk S, Meleshko D, Korobeynikov A, Pevzner PA. 2017. metaSPAdes: a new versatile metagenomic assembler. Genome Res 27:824-834.

62. Wu Y-W, Tang Y-H, Tringe SG, Simmons BA, Singer SW. 2014. MaxBin: an automated binning method to recover individual genomes from metagenomes using an expectation-maximization algorithm. Microbiome 2:26.

63. Kang DD, Froula J, Egan R, Wang Z. 2015. MetaBAT, an efficient tool for accurately reconstructing single genomes from complex microbial communities. PeerJ 3:e1165.

64. Huerta-Cepas J, Szklarczyk D, Heller D, Hernández-Plaza A, Forslund SK, Cook H, Mende DR, Letunic I, Rattei T, Jensen Lars J, von Mering C, Bork P. 2018. eggNOG 5.0: a hierarchical, functionally and phylogenetically annotated orthology resource based on 5090 organisms and 2502 viruses. Nucleic Acids Research 47:D309-D314.

65. Menzel P, Ng KL, Krogh A. 2016. Fast and sensitive taxonomic classification for metagenomics with Kaiju. Nature Communications 7: 1-9

66. Hartigan JA, Hartigan PM. 1985. The Dip Test of Unimodality. The Annals of Statistics 13:70-84.

Click here to view linked References

FIGURES

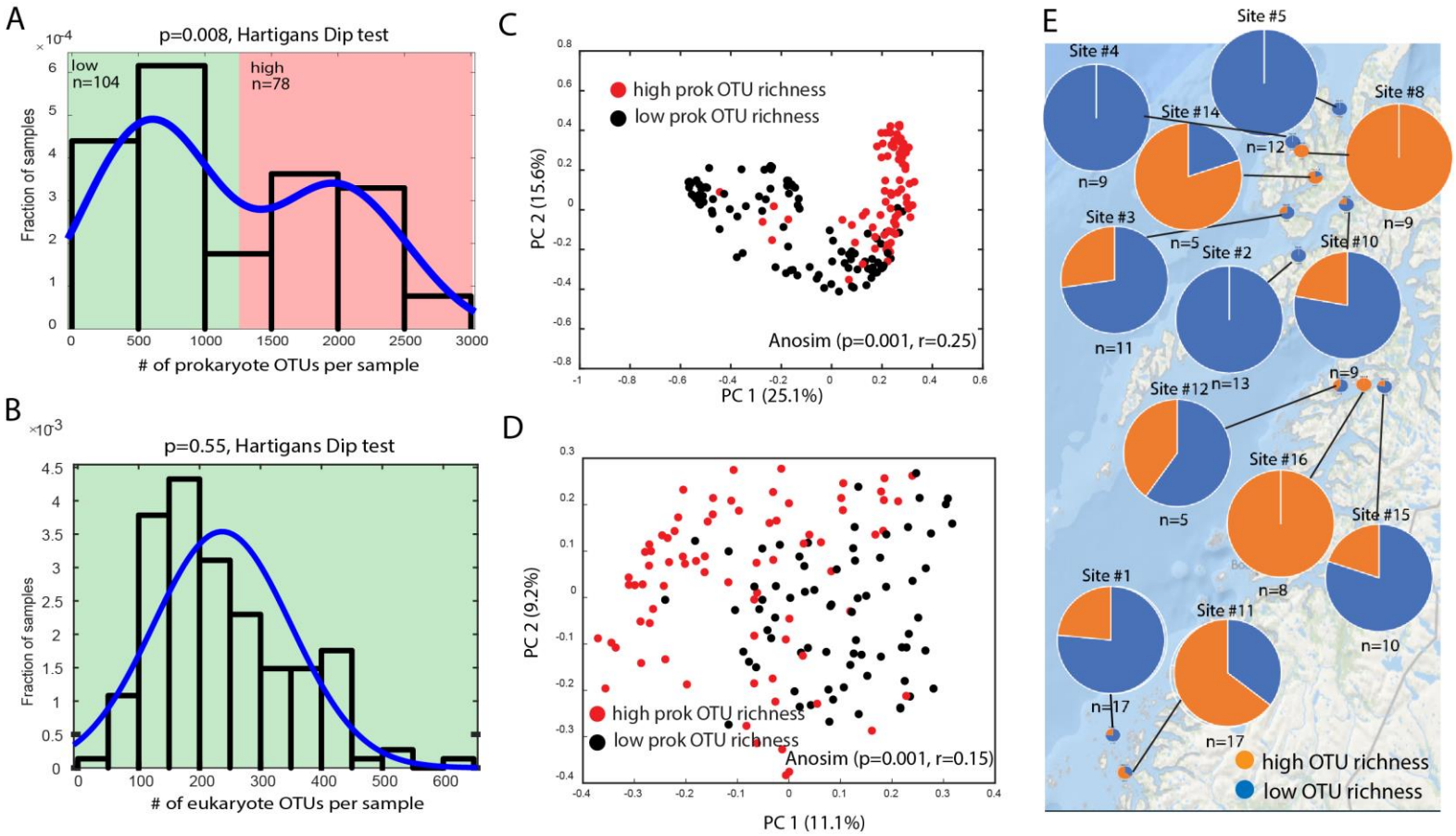

Figure 1. OTU richness distributions. (A) Prokaryote - and (B) eukaryote OTU richness density distribution, fitted by a smoothing spline curve. The scale represents the fraction of samples covered by the histogram bars. (C) Prokaryote and (D) eukaryote beta-diversity associations by Bray-Curtis distances. Anosim analyses were performed to determine the difference between the high and low OTU richness communities. (E) Distribution of the high and low OTU richness cluster across aquaculture for which geocoordinates were obtained.

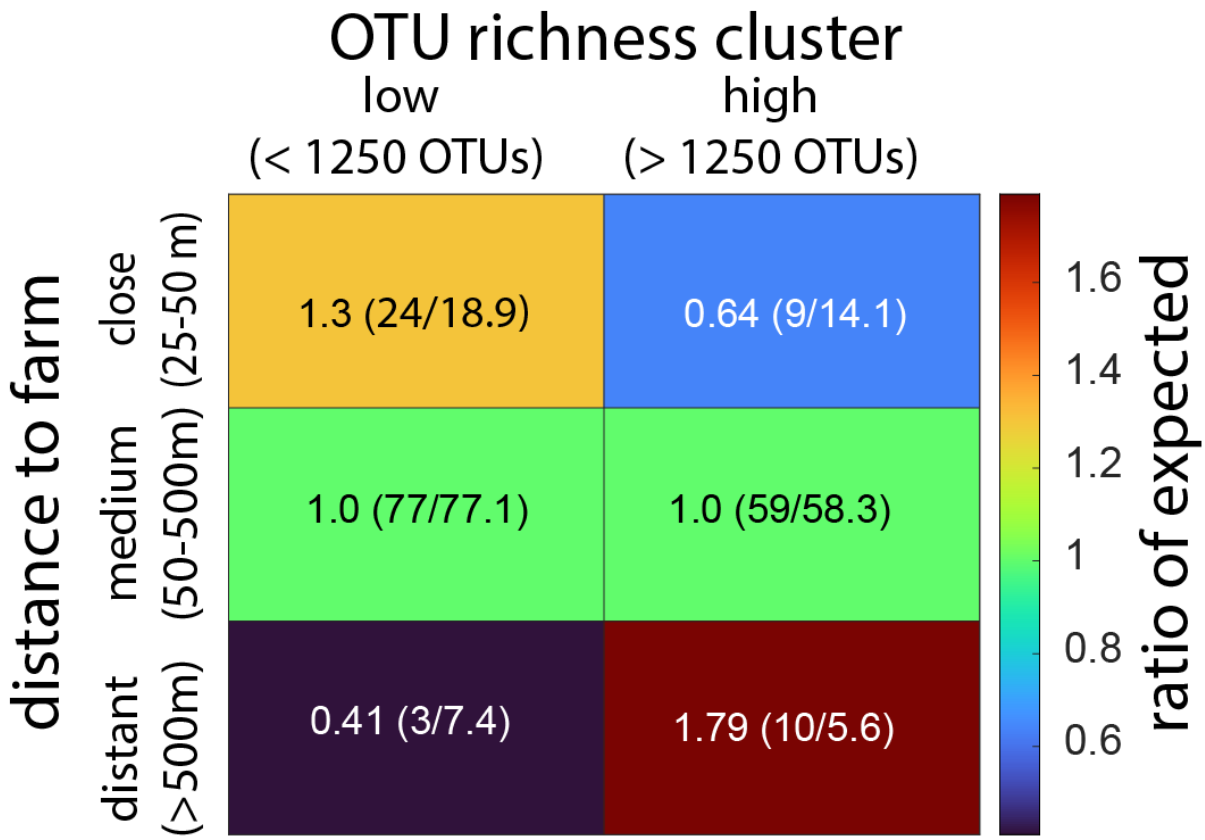

Figure 2. Association of high and low OTU richness cluster with aquaculture site. The association with distance to aquaculture sites is based on the ratio between observed and expected prevalence for the high and low OTU richness cluster. This is indicated by the color code and the numeric value of the ratio (actual numbers are shown in parentheses).

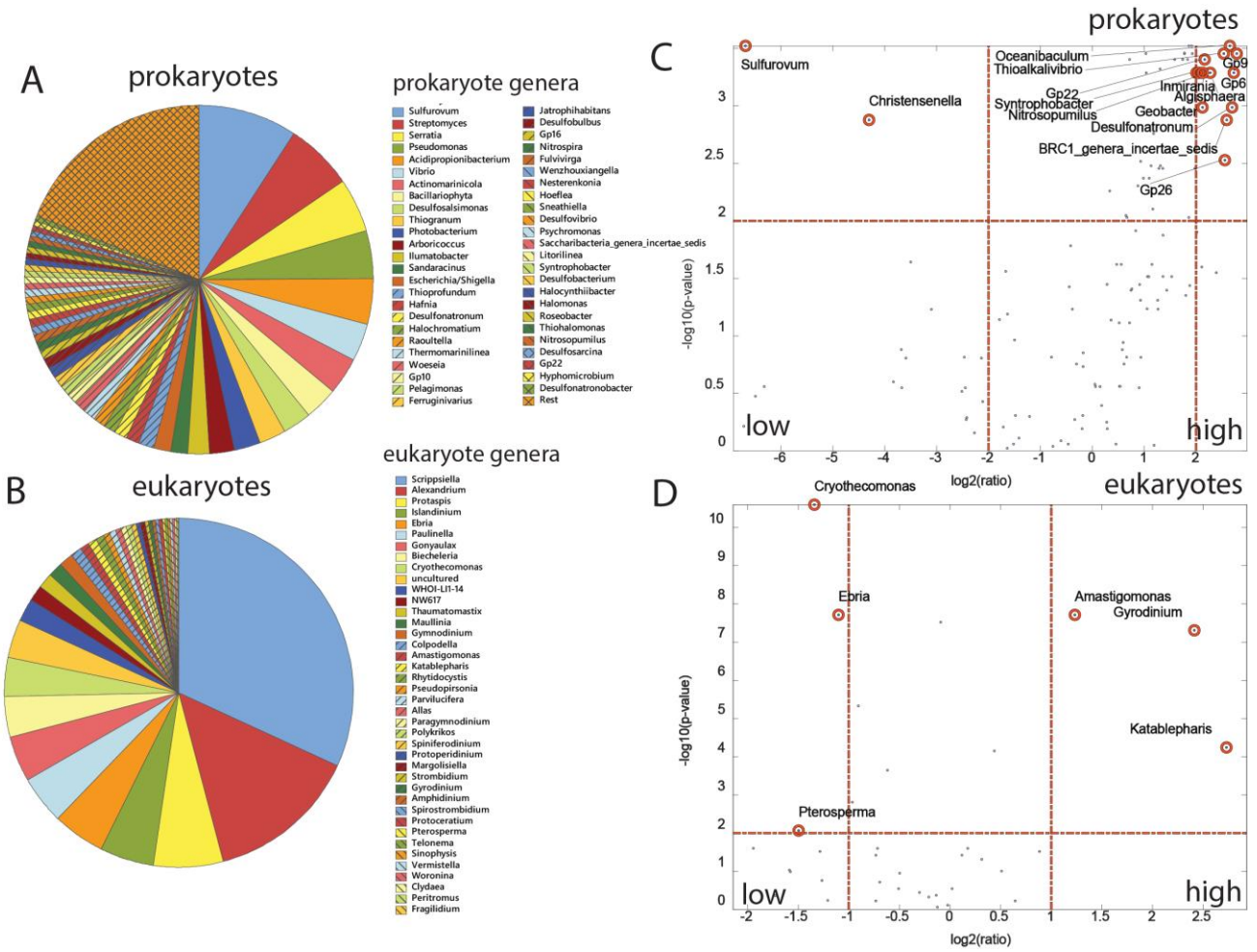

Figure 3. Genus composition and distribution. (A) Mean relative abundance of the most abundant (above 1 ‰.) prokaryote and (B) eukaryote genera. (C) Volcano plot for high and low prokaryote OTU richness association and (D) corresponding associations for eukaryotes. The non-enriched OTUs are shown as non-highlighted points, while the statistically enriched OTUs are highlighted with a red circle. Statistical testing was done using FDR corrected Kruskal-Wallis. The genera denoted as prokaryote were determined by 16S rRNA gene amplicon sequencing, while the genera denoted eukaryotes were determined by 18S rRNA gene amplicon sequencing.

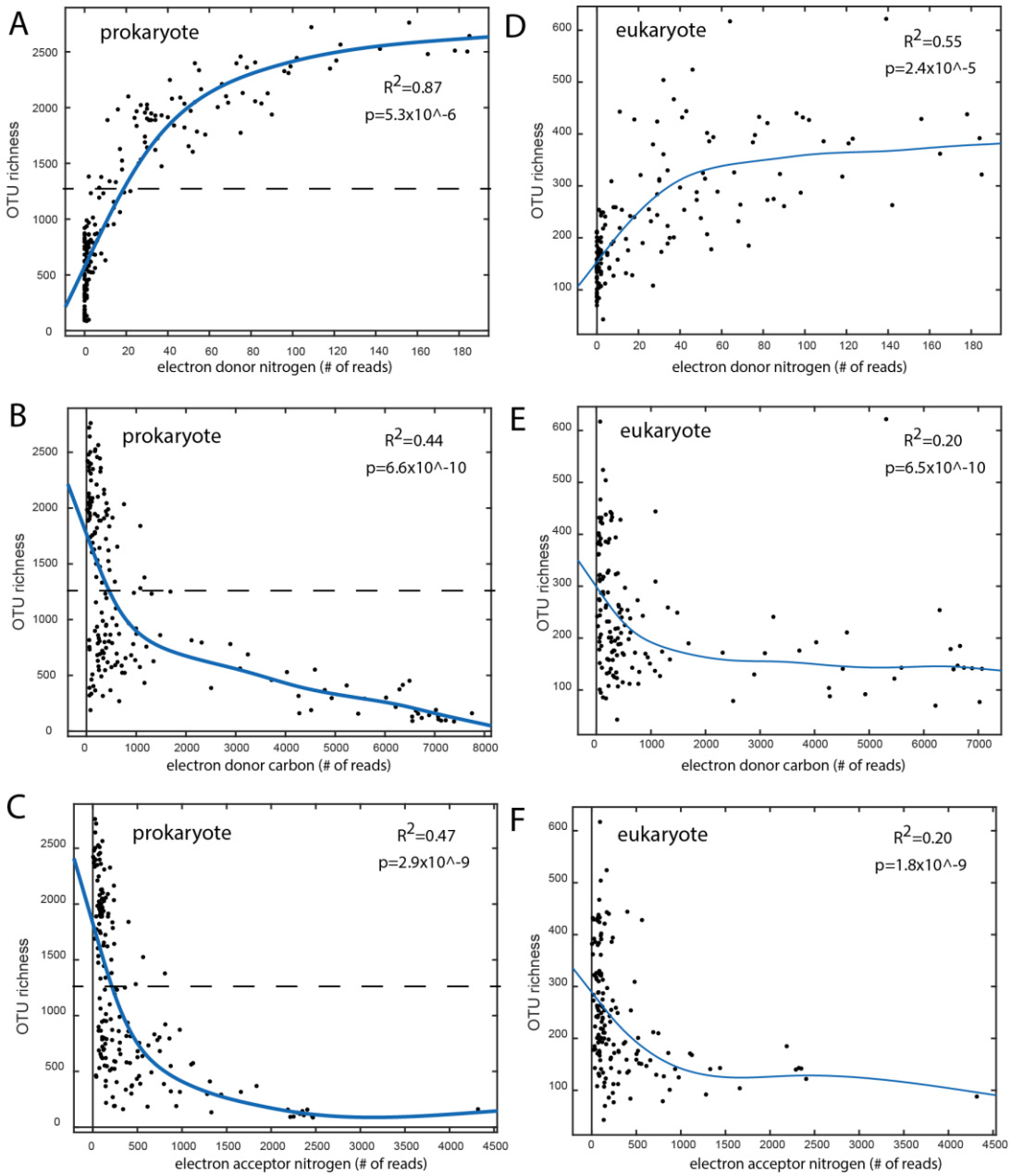

Figure 4. Functional associations of OTU richness for prokaryotes (A to c) and eukaryotes (D to F), with (A and D) nitrogen as electron donor, (B and E) carbon as electron donor, and (C and F) nitrogen as electron acceptor. Smoothing splines were used for regression analyses. Regressions were made with smoothing splines. Smoothness was empirically optimized. The horizontal dotted lines represent the threshold between the high- and low OTU richness cluster.

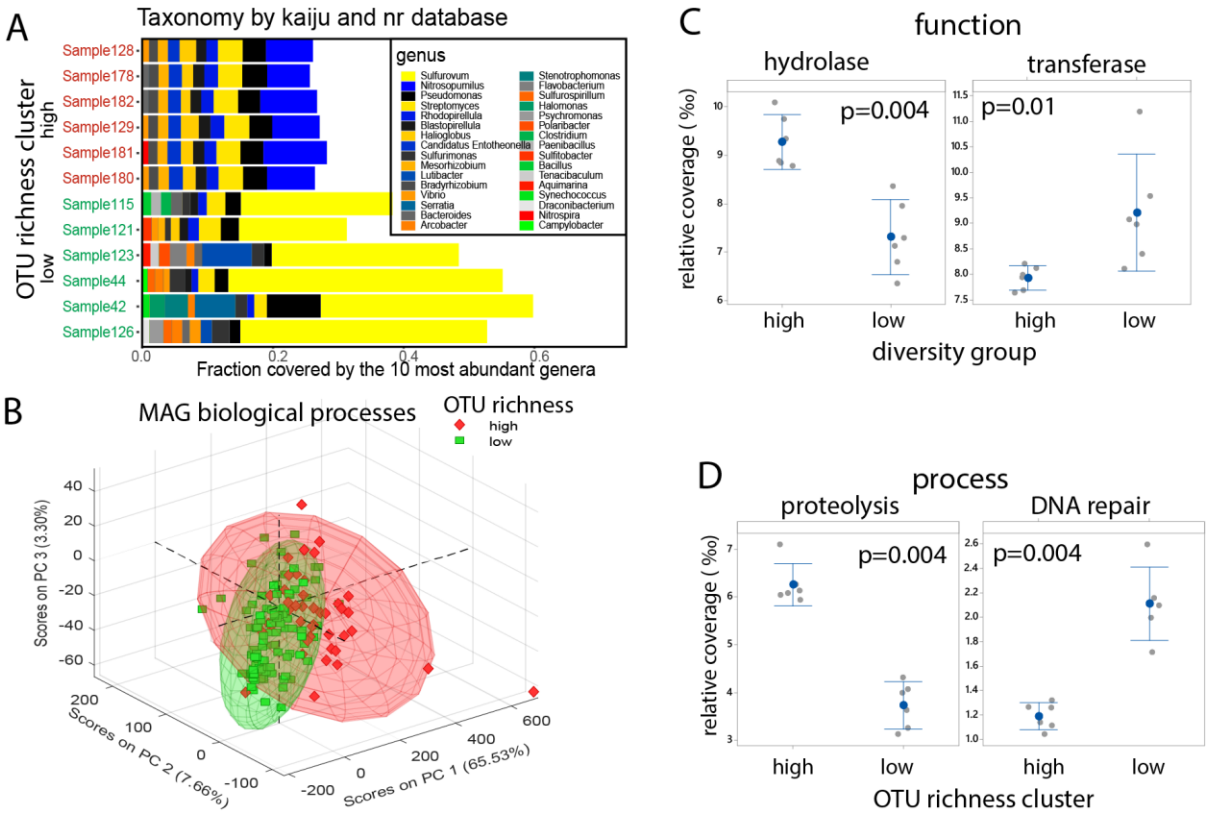

Figure 5. Taxonomic and functional analyses of high and low OTU richness cluster based on shotgun data. (A) Taxonomic classification was done using Kaiju with the nr database. The sample numbers correspond to that of Suppl. Table 1. Biological functions and processes were analyzed using GO classification. (B) Principal component analysis was used to visualize biological processes for all the derived MAG's (N=146). (C) Functions and (D) processes connected with the high and low OTU richness cluster. Statistical testing was done using the Kruskal-Wallis test.

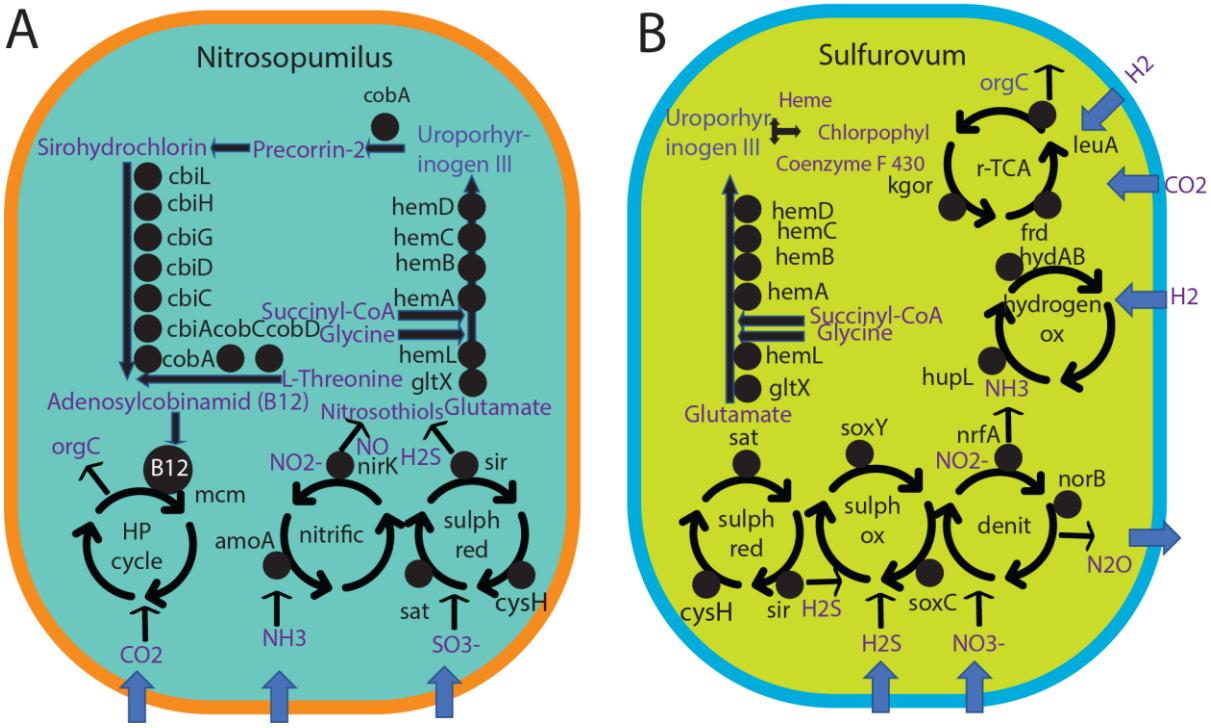

Figure 6. Deduced function for (A) *Nitrosopumilus* and (B) *Sulfurovum* based metagenome assembled pangenomes. Functional annotations were done using EggNOG. Black spheres represent genes, while purple text represents chemical compounds. Arrows represent transport in and out of the cells.

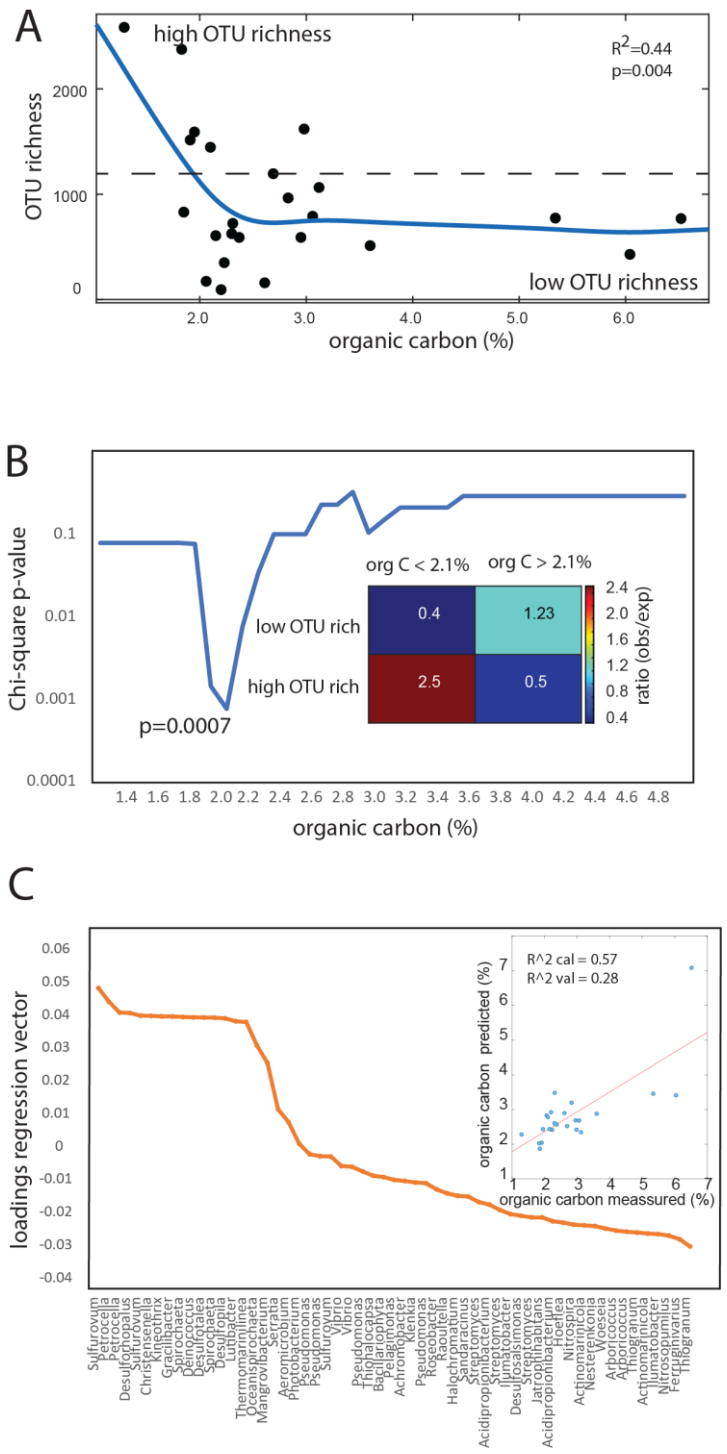

Figure 7. **Organic carbon level association with OTU richness. (**A) Scatter plot between OTU richness and organic carbon level, with smoothing spline regression and stippled border between high and low prokaryote OTU richness. (B) Total organic carbon levels in relation to OTU richness cluster**.** The graph shows p-values for the association of different thresholds of sediment organic carbon load, and the high and low OTU richness cluster (Chi-square test). The lowest p-value is marked, with the inserted panel showing the observed prevalence divided by the expected prevalence. (C) PLS regression analyses with organic carbon as response, and OTUs as predictors for 57 OTUs, selected based on a VIP score >2.

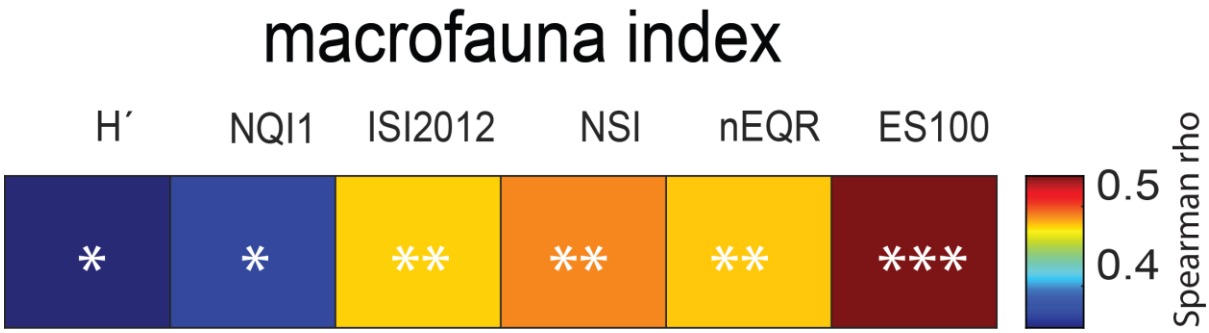

Figure 8. Correlation between macrofauna indexes and prokaryote OTU richness cluster. Spearman correlation between OTU richness cluster and macrofauna indexes. The asterisks indicate significant levels; * < 0.1, ** 0.05 and *** < 0.01.

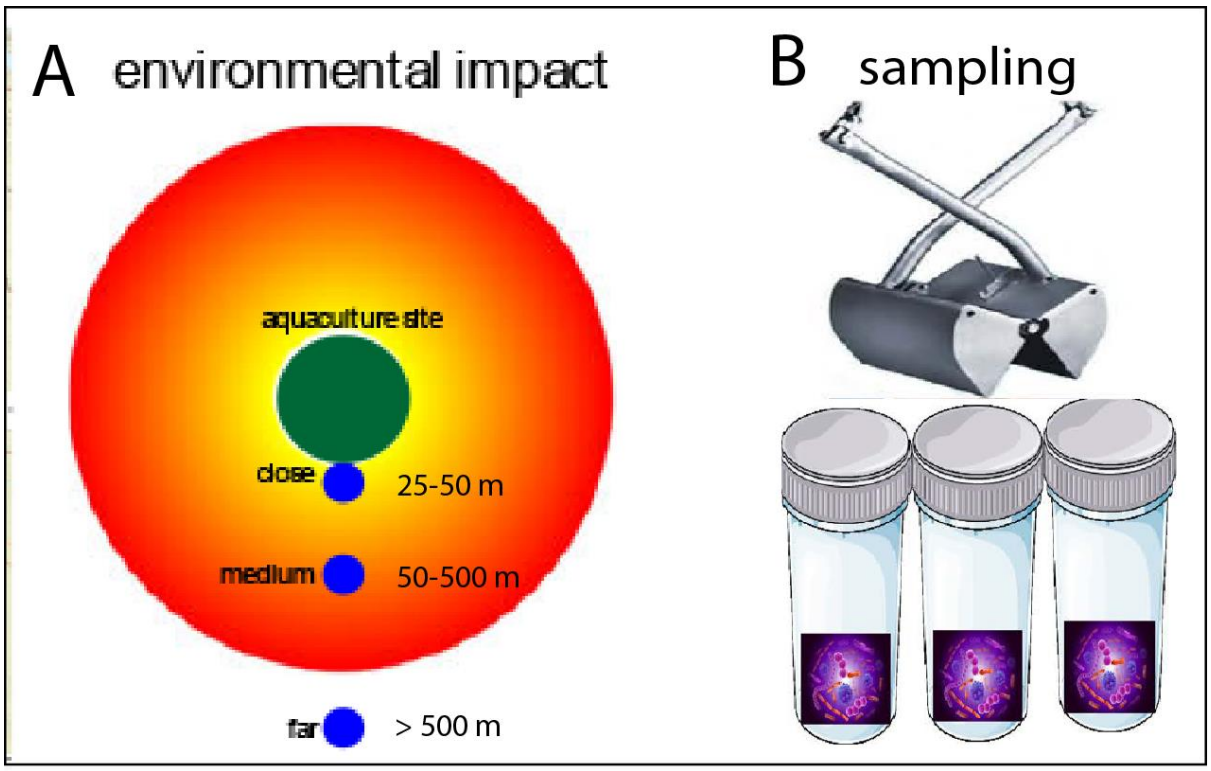

Figure 9. Distance from aquaculture site (A) and sampling strategy (B). (A) For each site, samples were collected close to the site (highest environmental impact), in an intermediate zone of impact (medium), sites with low expected impact (distant). Station C1 is positioned 30 m from the fish cages (close), which represents the border between the construction zone and the transitions zone for the aquaculture facility. Stations C2 to C5 are placed in regions expected to be affected (medium), while the reference stations are placed outside the regions expected to be affected by the aquaculture site. (B) A Van Veen grab was used for sampling. Three independent DNA extractions were done for each sampling site.

Declaration of interests

☒The authors declare that they have no known competing financial interests or personal relationships that could have appeared to influence the work reported in this paper.

☐The authors declare the following financial interests/personal relationships which may be considered as potential competing interests:

Credit Author Statement

R. Pettersen: Investigation; Methodology; Conseptualization

, I. Ormaasen: Investigation; Methodology;

I. L. Angell: Investigation; Methodology;

N. B. Keeley: Writing

A. Lindseth: Conceptualization

L. Snipen: Investigation; Methodology;

K. Rudi: Investigation; Methodology; Conceptualization, Writing

All authors contributed with commenting and revision